

Positron-impact electronic excitations and mass stopping power of H₂R. Utamuratov,^{*} D. V. Fursa, N. Mori, A. S. Kadyrov, and I. Bray*Curtin Institute for Computation and Department of Physics and Astronomy, Curtin University, Perth, Western Australia 6102, Australia*

M. C. Zammit

Theoretical Division, Los Alamos National Laboratory, Los Alamos, New Mexico 87545, USA

(Received 11 January 2019; published 29 April 2019)

Positron-impact electronic excitation cross sections, mean excitation energies, and mass stopping power of the H₂ molecule have been calculated for energies from 10 eV up to 2 keV using the convergent close-coupling method that utilizes single- and two-center expansions. Results are compared to previous studies. Application of Bragg's rule of stopping power additivity is discussed by comparing results obtained for atomic (H) and molecular (H₂) targets for positron impact.

DOI: [10.1103/PhysRevA.99.042705](https://doi.org/10.1103/PhysRevA.99.042705)**I. INTRODUCTION**

A positron is the most abundant and accessible antimatter particle. Studies of its interactions with matter are of high interest in many areas of practical applications and fundamental science. Positron microscopes [1] in material science and the positron-emission tomography scanners [2] in medical diagnostics are the most well-known practical applications of positrons. Such technologies require a detailed understanding of positron collision processes to improve their accuracy and reliability. Positron collisions with atoms and molecules can also help in resolving a number of fundamental problems such as unknown sources of positron jets in the center of our galaxy [3], missing antimatter [4], spectroscopic and gravitational properties of antimatter [5,6], and very recent observations of positron clouds produced during thunderstorms [7].

Molecular hydrogen, H₂, is the most abundant molecule in the Universe, particularly in the interstellar media [8]. Studies of positron-H₂ collisions are of high interest and a good starting point for theoretical models. The existence of positronium (Ps) formation in such collisions adds more interest and complexity for theoretical studies. Because the positron is the antimatter counterpart of the electron, comparative analysis of collision dynamics for positron and electron projectiles can reveal some interesting physics. While the electron-H₂ system has been studied extensively both experimentally [9] and theoretically ([10] and references therein), positron studies are somewhat behind. This was mainly because of the above-mentioned complexities for theoretical approaches and lack of low-energy high-intensity positron beams for experimental studies. However, recent developments in experimental techniques of positron traps [11] have motivated more intensive theoretical studies of positron collisions while rapidly increasing computing power is enabling more sophisticated theoretical approaches.

In quantifying the collision processes, a particular quantity of interest is the stopping power, because of its use in

modeling projectile transport through matter. Accurate information on the stopping power is essential in the interpretation of experiments, transport modeling, and particularly in practical applications such as medical dosimetry. Previous calculations of the positron stopping power of molecules relied on high-energy approximations using the Bethe formula [12,13] combined with Bragg's additivity rule [14]. In these calculations, the difference between the positrons and electrons was taken into account via wave-function symmetry and polarization effects. However, the other aspects of collision dynamics such as Ps formation and direct annihilation were neglected. These approaches are usually applicable at high collision energies (>1000 eV).

Many applications require accurate stopping power values at low and intermediate energies [15–17] for modeling the projectile's entire path through media. Attempts were made to extend semiclassical calculations of the stopping power to lower energies by using the generalized oscillator strength model [18]. However, an accurate estimate of the stopping power at low and intermediate energies requires calculations of cross sections for all important energy-loss channels such as excitation, ionization, and Ps formation. This in turn requires large-scale multichannel calculations with realistic accounts of the target structure and interaction potentials.

Several theoretical studies of the e⁺-H₂ system have been reported over the last few decades. Lodge *et al.* [19] calculated low-energy elastic scattering cross sections and annihilation rates using polarized potentials. Ray *et al.* [20] applied the first Born approximation (FBA) combined with the molecular Jackson-Schiff approach to estimate Ps formation in the ground and arbitrary *s*-states. Armour *et al.* [21] used the Kohn variational method to calculate annihilation rates and total cross sections. Biswas *et al.* [22] applied the FBA to calculate the cross sections for Ps formation in *n* = 2 states for impact energy range 30-1000 eV. Mukherjee *et al.* [23] used a close-coupling approach that included two electronic and three rotational states to calculate elastic, electronic and rotational excitation cross sections. Campeanu and coworkers [24–26] applied the distorted-wave Born and molecular 3C

^{*}r.utamuratov@curtin.edu.au

approximations to calculate integrated and triple differential cross sections for ionization of H₂ and obtained good agreement with experimental data [27,28]. The Schwinger multi-channel method [29,30] was used to calculate target excitation cross sections at low impact energies. Zhang *et al.* [31,32] applied the variational and R-matrix methods to calculate annihilation rates and elastic scattering cross sections at impact energies below the Ps-formation threshold. All of the above-mentioned theoretical studies of positron-H₂ collisions have either utilized model potentials or included only the ground and a few excited states. This is not sufficient to accurately estimate the stopping power in the low- and intermediate-energy regions.

Recent experiments [33–35] measured elastic scattering, grand total, Ps-formation, ionization, and first excitation cross sections. However, there is still a lack of reliable and sufficient data sets on positron-impact excitation cross sections and positron stopping power of H₂. This warrants further theoretical and experimental studies of the positron-H₂ collision system.

Recently, we have reported successful application of the convergent close-coupling (CCC) method to positron, electron, and heavy-ion scattering from H₂ molecules [36–39]. Both single- and two-center approaches have been used within the CCC method. This has allowed a check of the internal consistency of the method and also allowed us to obtain all cross sections of interest, including charge transfer, ionization, and stopping power [40–43].

In this paper, we present results for positron-impact electronic excitations and the mass stopping power of H₂ calculated within the CCC method [37,38]. At low and intermediate energies our results explicitly include Ps-formation channels while an account of a large number of H₂ excitation and ionization channels is particularly important at high energies. The positron-impact excitation and the mass stopping power results are compared against electron-scattering results [44,45] and the differences arising from the two-center nature and absence of electron exchange are discussed. Additionally, we check Bragg's additivity rule for positron stopping by comparing results for atomic (H) and molecular hydrogen (H₂).

II. FORMALISM

Details of the single-center and two-center CCC methods applied to positron collisions on H₂ have been presented in our previous reports [37,38]. Here we present only a brief description. Following the CCC method [45–48] the Born-Oppenheimer approximation is applied to the total scattering wave function of the e⁺-H₂ system. A two-center close-coupling expansion is then performed for the total wave function as

$$\begin{aligned} \Psi_i^{N(+)}(\mathbf{r}_0, \mathbf{r}_1, \mathbf{r}_2) &= \sum_{n=1}^{N_\alpha} f_n^{N_\alpha(+)}(\mathbf{r}_0) \Phi_n^{N_\alpha}(\mathbf{r}_1, \mathbf{r}_2) \\ &+ (1 + P_{12}) \sum_{n=1}^{N_\beta} g_n^{N_\beta(+)}(\mathbf{R}_{01}) \psi_n^{N_\beta}(\boldsymbol{\rho}_{01}) \psi_{\text{ion}}(\mathbf{r}_2), \quad (1) \end{aligned}$$

where $N = N_\alpha + N_\beta$ is the total number of basis states with N_α and N_β denoting the target and Ps basis sizes, respectively; (+) indicates outgoing boundary conditions; indices 0, 1, and 2 denote a positron and two electrons; vector $\mathbf{R}_{0j} = (\mathbf{r}_0 + \mathbf{r}_j)/2$ indicates the positions of the Ps center relative to the residual ion and $\boldsymbol{\rho}_{0j} = \mathbf{r}_0 - \mathbf{r}_j$ is the relative coordinate of Ps. The target wave functions $\Phi_n^{N_\alpha}$ and the wave function of the residual ion ψ_{ion} (the ground state of H₂⁺) are calculated at the average internuclear distance of the H₂ ground state, $R = 1.448 a_0$, with R being implicit in Eq. (1). The above expansion assumes the target wave functions $\Phi_n^{N_\alpha}$ to be already symmetrized (for singlet states) and therefore P_{12} , the coordinate-space interchange operator, is applied to only the Ps part of the expansion. Also in positron scattering from the ground state of H₂ we only consider singlet states, as spin interactions between the positron and electrons are ignored.

The total wave-function expansion given in Eq. (1) is the starting point in all close-coupling methods. The single-center approach assumes $N_\beta = 0$ and is applicable at energies below the Ps-formation and above the single-ionization thresholds. The single-center CCC method uses relatively large N_α combined with large angular momentum l orbitals to produce convergent results. It has been successfully applied to both light and heavy projectile scattering from various targets [36]. The two-center expansion with $N_\alpha > 0$ and $N_\beta > 0$ is able to explicitly account for Ps-formation channels and is applicable at all impact energies.

In the CCC method, using the expansion in Eq. (1), Schrödinger's equation is transformed into momentum-space coupled-channel equations for the transition matrix elements, from which all observables such as cross sections of various transitions can be obtained.

A. Stopping power

Previously we have reported the integrated cross sections (ICS) for elastic scattering, grand total, and electron loss obtained with the single-center CCC approach [37,49]. The direct-ionization and Ps-formation cross sections have been calculated within the two-center CCC method [38]. The same calculations have also produced results for target excitation cross sections. In this paper we use these results to calculate the mass stopping power for positrons traversing through H₂ gas. The mass stopping power is defined as the positron energy loss per unit path length per unit density with the following relation:

$$Q_{\text{SP}} \equiv -\frac{1}{\rho} \frac{dE}{dx} = \frac{N_A}{M} \sigma_{\text{SP}}, \quad (2)$$

where N_A is the Avogadro number, ρ is the density of the target, M is the molar mass, and σ_{SP} is the stopping cross section per collision.

The CCC calculations of the stopping cross section σ_{SP} for electrons were reported by Fursa *et al.* [44]. We can define σ_{SP} for positrons in a similar way with some additional modifications. The stopping cross section for positrons will have two separate contributions:

$$\sigma_{\text{SP}} = \sigma_{\text{SP}}^{\text{H}_2} + \sigma_{\text{SP}}^{\text{Ps}}, \quad (3)$$

where $\sigma_{\text{SP}}^{\text{H}_2}$ is the contribution due to target excitation and ionization and $\sigma_{\text{SP}}^{\text{Ps}}$ is the contribution due to Ps formation. For brevity, we have omitted an explicit dependence on the incident positron energy E in all equations. The target contribution is the same as for electrons:

$$\sigma_{\text{SP}}^{\text{H}_2} = \sum_{n=1}^{N_\alpha} (\varepsilon_n - \varepsilon_0) \sigma_n, \quad (4)$$

where N_α is the total number of target states included in the calculations, n denotes the channel number, σ_n is the excitation cross section of the n th state with energy ε_n ; the ground state of the target is indexed as $n = 0$ with energy ε_0 .

The Ps contribution requires cross sections of Ps formation and Ps breakup due to Ps collisions with H_2 . In this paper we ignore Ps breakup contribution, which requires calculations of Ps scattering from H_2 . Instead, as suggested by the Ore model of Ps formation [50], we assume that all Ps formed above the target ionization threshold quickly break up in subsequent collisions. With this assumption, the energy loss of positrons due to Ps formation can be calculated from the energy conservation. We denote the initial and final kinetic energies of the positron as K_i and K_f , respectively. In the Ps, the positron will have half of the kinetic energy available after Ps breakup:

$$K_f = \frac{1}{2}(K_i - I_{\text{H}_2}), \quad (5)$$

where I_{H_2} is the ionization energy of the target. Then the energy loss of the positron is

$$\Delta K = K_i - K_f = \frac{1}{2}(K_i + I_{\text{H}_2}). \quad (6)$$

As a result, we can write the Ps contribution to the stopping power cross section as

$$\sigma_{\text{SP}}^{\text{Ps}} = \Delta K \sum_{n=1}^{N_\beta} \sigma_n = \Delta K \sigma_{\text{Ps}}, \quad (7)$$

where N_β is total number of Ps states and n denotes the Ps-formation channel number; σ_n is the cross section of Ps formation in the n th state and σ_{Ps} is the total Ps-formation cross section.

A few other parameters related to stopping power are also used in the literature. One such parameter is \bar{E} —the mean excitation energy per collision, defined as the ratio of total stopping power cross section σ_{SP} to total inelastic cross section σ_{inel} :

$$\bar{E}_{\text{total}} = \frac{\sigma_{\text{SP}}}{\sigma_{\text{inel}}}. \quad (8)$$

The total inelastic cross section σ_{inel} is a sum of excitation, ionization, and Ps-formation cross sections.

Note that, for positron collisions, this definition of \bar{E}_{total} also contains contribution from Ps-formation processes. Therefore we refer to \bar{E}_{total} , defined in Eq. (8), as the total mean excitation energy. In order to compare with the electron-scattering case we also calculate the target contribution to the mean excitation energy \bar{E}_{target} that corresponds to only target excitations without the Ps-formation contribution:

$$\bar{E}_{\text{target}} = \frac{\sum_{n=1}^{N_\alpha} (\varepsilon_n - \varepsilon_0) \sigma_n}{\sum_{n=1}^{N_\alpha} \sigma_n} = \frac{\sigma_{\text{SP}}^{\text{H}_2}}{\sigma_{\text{inel}}^{\text{H}_2}}, \quad (9)$$

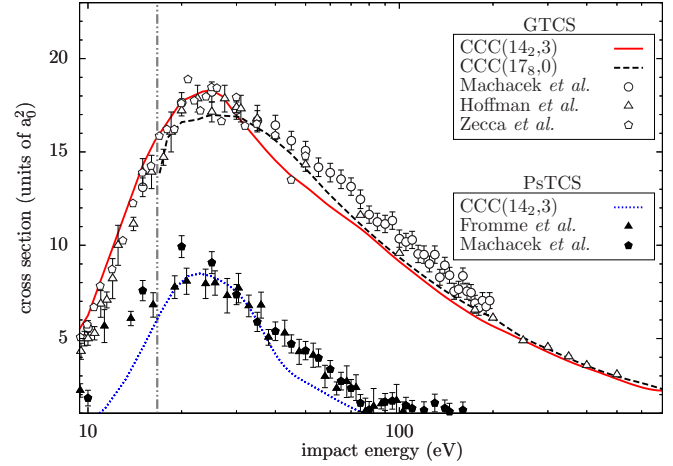


FIG. 1. Grand total and Ps-formation cross sections. The single- and two-center CCC results are denoted as CCC(17₈, 0) and CCC(14₂, 3), respectively. Experimental data for GTCS are due to Machacek *et al.* [35], Hoffman *et al.* [51], and Zecca *et al.* [34]. Experimental data for Ps formation are due to Machacek *et al.* [35] and Fromme *et al.* [52]. The vertical bar shows the single ionization energy threshold of H_2 .

where the total target inelastic cross section $\sigma_{\text{inel}}^{\text{H}_2}$ is a sum of all cross sections σ_n for excitation of target bound and continuum states:

$$\sigma_{\text{inel}}^{\text{H}_2} = \sum_{n=1}^{N_\alpha} \sigma_n. \quad (10)$$

The mass stopping power calculated in this paper refers to the energy loss due to electronic excitations and ionization of H_2 , and Ps formation in the ground and excited states (assuming the residual ion is in the ground state). As we use the fixed-nuclei approximation, vibrational and rotational excitations are not calculated explicitly. We also neglect direct annihilation of positrons with target electrons since at the energy range we are considering its contribution is orders of magnitude smaller and also the direct annihilation lifetime is much larger than the stopping time. Both rovibrational excitations and direct annihilation are of importance only at low energies and will be considered elsewhere. The dissociative processes are accounted for indirectly in the present technique, as in the fixed-nuclei approximation the calculated excitation cross sections describe scattering to all rovibrational levels of electronic excited states, including dissociation.

B. Results

To evaluate the stopping cross section from Eqs. (3)–(7) we first need to calculate cross sections of the main energy-loss channels. We have previously reported the convergence studies for the grand total, the total ionization, and the Ps-formation cross sections [37,38,53] for H_2 at the mean internuclear separation of $R = 1.448 a_0$. Figure 1 shows the grand total (GTCS) and Ps-formation cross sections obtained within the single- and two-center CCC approaches and compares them with experimental data [34,35,51,52]. The single-center CCC results [37] above the single-ionization threshold were obtained using a large H_2 basis of 1013 states with $l_{\text{max}} = 8$,

TABLE I. Two-electron energies of the H_2 singlet electronic states obtained in the single-center calculations, model (a) [37], and the two-center calculations, model (b) [38], for the internuclear distance $R = 1.4 a_0$. Comparisons are made with accurate calculations [54–59].

H ₂ two-electron energies (atomic units)			
State	Ref.	Model (a)	Model (b)
$X^1\Sigma_g^+$	-1.174 [54]	-1.169	-1.147
$B^1\Sigma_u^+$	-0.706 [55]	-0.702	-0.689
$EF^1\Sigma_g^+$	-0.692 [56]	-0.689	-0.677
$C^1\Pi_u$	-0.689 [55]	-0.686	-0.674
$B^1\Sigma_u^+$	-0.629 [55]	-0.627	-0.601
$GK^1\Sigma_g^+$	-0.626 [56]	-0.625	-0.612
$I^1\Pi_g$	-0.626 [57]	-0.625	-0.612
$J^1\Delta_g$	-0.625 [58]	-0.624	-0.611
$H^1\Sigma_g^+$	-0.624 [59]	-0.623	-0.585
$D^1\Pi_u$	-0.624 [55]	-0.622	-0.592

which we denote as CCC(17₈,0). The CCC calculations have shown that the first-order Born approximation is valid at impact energies above 200 eV for positron scattering (from H₂). Therefore, the results of the above model were substituted with the Born results obtained with an even larger basis of 2491 states and $l_{\max} = 8$. This will allow a more accurate representation of the continuum at high energies. At impact energies above the single-ionization threshold, the single-center calculations can also account for Ps-formation process indirectly through excitations to positive-energy pseudostates with higher angular momenta.

The two-center CCC results [38] have been obtained using only 139 states of H₂ with $l_{\max} = 2$ and the three lowest eigenstates of Ps, which we denote as CCC(14₂,3). The single-center and two-center CCC results for the GTCS are in good agreement above 30 eV and confirm the internal consistency of the two methods and calculation models. The Ps-formation cross sections are peaked at about 20 eV and only slightly underestimate experimental data above 30 eV.

In this paper, we join the two results, by using the two-center CCC results up to 30 eV and the single-center CCC results at higher energies. The reason for such an approach is that the single-center CCC calculations have achieved a better convergence for high excited states of H₂, which are important to obtain accurate stopping cross sections. The two-center calculations have a relatively small basis size and therefore cross sections for higher excited states were not as accurate. This can be seen in Table I, which presents two-electron energies of H₂ obtained with the models used in our calculations and accurate calculations [54–59] for comparison. The models used in the single- and two-center calculations are denoted as “model (a)” and “model (b),” respectively. Comparison with accurate structure calculations [54–59] shows that model (a) has produced accurate energies for the ground and excited states up to the $D^1\Pi_u$ state. The model (b) results are within 2% of the accurate results [54–59] for the ground and first excited states, but accuracy decreases for higher states, which are important to obtain accurate excitation and stopping power cross sections.

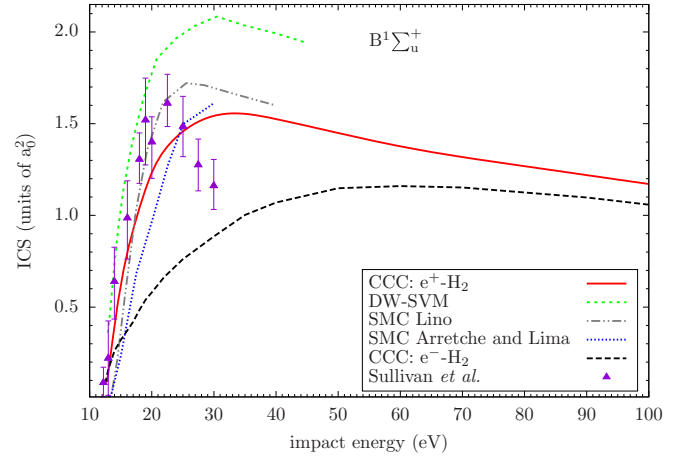


FIG. 2. ICS for positron-impact excitation of the $B^1\Sigma_u^+$ state. The DW-SVM calculations are due to Weiss *et al.* [60], the two-state SMC results are due to Lino [61], and the five-state SMC results are due to Arretche and Lima [29]. The experimental data are due to Sullivan *et al.* [33]. The CCC results [10] for electron impact are shown for comparison.

The ICS for the excited $B^1\Sigma_u^+$ state are presented in Fig. 2. The CCC results are compared with previous calculations [23,30,60] which did not include Ps-formation channels. Our results are generally in good agreement with the only available experimental data obtained by Sullivan *et al.* [33]. The only noticeable disagreement is at the 20-eV peak and the behavior of the cross sections above 25 eV, where the experimental values are decreasing while the CCC results are not. The calculations of Weiss *et al.* [60] using the distorted-wave Schwinger variational method (DW-SVM) are consistently higher than the experimental and CCC results. The two-state Schwinger multichannel (SMC) method calculations of Lino [61] are in good agreement with the experiment and the current results up to 20 eV. The SMC calculations of Arretche and Lima [29] which utilize five states underestimate the experiment and the current results below 25 eV. Comparison with the CCC results for the e^-H_2 system [10] shows that

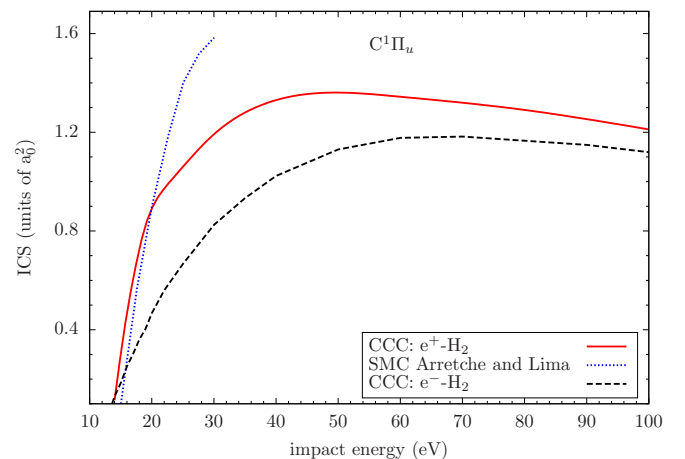


FIG. 3. ICS for positron-impact excitation of the $C^1\Pi_u$ state. The SMC calculations are due to Arretche and Lima [29]. The CCC results [10] for electron impact are also shown for comparison.

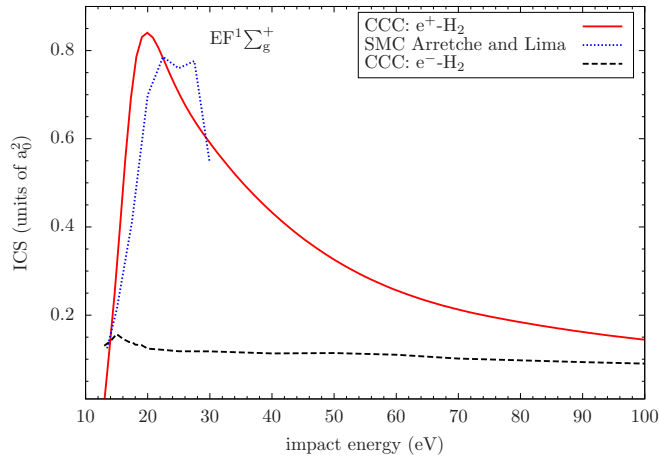


FIG. 4. ICS for positron-impact excitation of the $EF^1\Sigma_g^+$ state. The five-state SMC calculations are due to Arretche and Lima [29]. The CCC results [10] for electron impact are also shown for comparison.

positron-impact excitation cross sections are higher than for electron impact at intermediate energies.

Figure 3 presents ICS for positron-impact excitations to the $C^1\Pi_u$ state. These cross sections are similar in shape and magnitude to the $B^1\Sigma_u^+$ state presented in Fig. 2. The SMC calculations of Arretche and Lima [29] are higher than the CCC results above 20 eV. As in the previous figure, the CCC results for electron-impact excitation of the $C^1\Pi_u$ state are consistently lower than for positrons.

The ICS for positron-impact excitation of the $EF^1\Sigma_g^+$ state are shown in Fig. 4. Comparisons are made with results of the SMC calculations of Arretche and Lima [29]. The results of two methods differ from each other, only agreeing in terms of the scale of cross-section values. The CCC results for electron-impact excitations of the $EF^1\Sigma_g^+$ state are substantially lower than for positrons at intermediate energies.

Figure 5 presents positron-impact cross sections to some of the higher excited states, namely, $B^1\Sigma_u^+$, $D^1\Pi_u$, $GK^1\Sigma_g^+$,

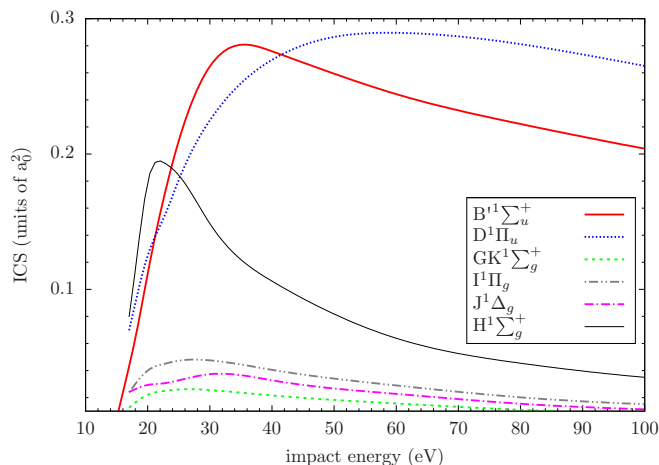


FIG. 5. ICS for positron-impact excitations of the higher excited states ($B^1\Sigma_u^+$, $D^1\Pi_u$, $GK^1\Sigma_g^+$, $I^1\Pi_g$, $J^1\Delta_g$, and $H^1\Sigma_g^+$).

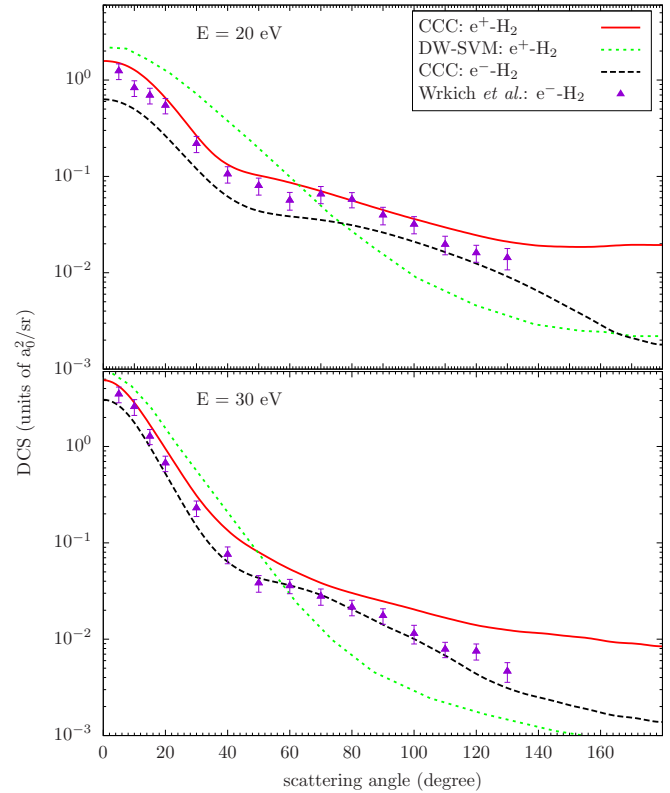


FIG. 6. DCS for the $B^1\Sigma_u^+$ excitation at impact energies of 20 and 30 eV. The DW-SVM calculations are due to Weiss *et al.* [60]. The electron-impact DCS are due to the measurements of Wrkich *et al.* [62] and the CCC calculations [10] are shown for comparison.

$I^1\Pi_g$, $J^1\Delta_g$, and $H^1\Sigma_g^+$. To the best of our knowledge, there are no other theoretical or experimental results for these cross sections. Cross sections of any excited states can be calculated within the CCC method, provided a sufficiently large basis is used. The convergence rate of cross sections of high excitation states can be slow, even though the sum of all cross sections converges relatively fast.

Studies of particle transport in media would benefit from availability of angle differential cross sections (DCS). As an example, the DCS of the $B^1\Sigma_u^+$ state are given in Fig. 6 for impact energies of 20 and 30 eV. We compare our results with recent theoretical results obtained using the DW-SVM by Weiss *et al.* [60]. In the absence of any experimental measurements of DCS for positrons, we compare with the CCC results [10] and experimental data by Wrkich *et al.* [62] for electron scattering on H_2 . Surprisingly, our results for positron scattering are in good agreement with the experimental data for electrons, particularly at forward-scattering angles. This is due to the fact that for these energies the DCS at forward-scattering angles are dominated by contributions from higher partial waves, for which rearrangement and electron exchange are negligible. The CCC results for electrons are lower than for positrons at all angles as expected from the ICS comparison in Fig. 2.

Calculations of the target excitation and ionization cross sections allow us to obtain the target mean excitation energy \bar{E}_{target} for positron impact using Eq. (9). Results are shown

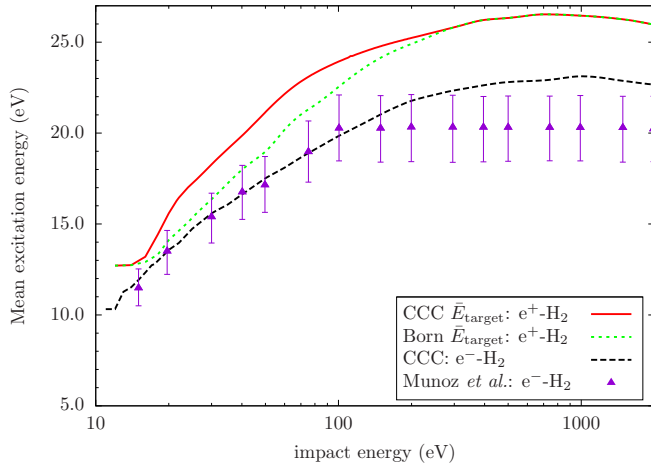


FIG. 7. Mean excitation energies. The experimental data for e^- -H₂ are due to Munoz *et al.* [63]. The CCC calculations for e^- -H₂ are due to Fursa *et al.* [44].

in Fig. 7 and compared with the first-order Born approximation which utilizes plane waves for the projectile. It can be seen that the first-order Born approximation is applicable to positron scattering above 200 eV. Note that the Born calculations presented here include only singlet states of H₂ and therefore only apply to positron scattering. The electron-impact mean excitation energies extracted from the experimental data of Munoz *et al.* [63] and the CCC calculations by Fursa *et al.* [44] are also presented for comparison. We find that the target mean excitation energy for positron impact is larger than for electron impact at low and intermediate energies. The larger mean excitation energy leads to larger stopping power, which means that positrons lose their energy faster and as a result travel less distance than electrons with the same initial kinetic energy.

At impact energies near and above 1000 eV, both Ps formation and electron exchange will be negligible and therefore the CCC results of positron and electron impact are expected to be the same. However, the CCC calculations for e^- -H₂ [44] are about 12% lower than for positrons even at 1000 eV and above. This indicates that the basis of 491 states with $l_{\max} = 3$ used for the e^- -H₂ calculations was not sufficiently large to account for high-energy continuum states. Therefore, the CCC results for the e^- -H₂ proved to be about 15% larger than the experimental data of Munoz *et al.* [63] at higher energies. However, calculations of \bar{E}_{target} for the e^- -H₂ with use of Eq. (9) do not exactly compare the quantity measured in the experiments of Munoz *et al.* [63]. The experimental \bar{E} has been derived from the energy-loss spectra [63,64] of the electron beam. Due to indistinguishability of electrons, both incident and ejected electrons contribute to the measured spectra. On the other hand, the calculations of \bar{E}_{target} with Eq. (9) assume energy loss of the incident projectile.

In order to calculate the energy-loss spectra of the beam, one should use the single differential cross sections (SDCS) of the target ionization to subtract the energy-loss signal from the secondary electrons. The method of calculating the SDCS for e^- -H₂ and using it to investigate the above-mentioned discrepancies in \bar{E} values will be the subject of further

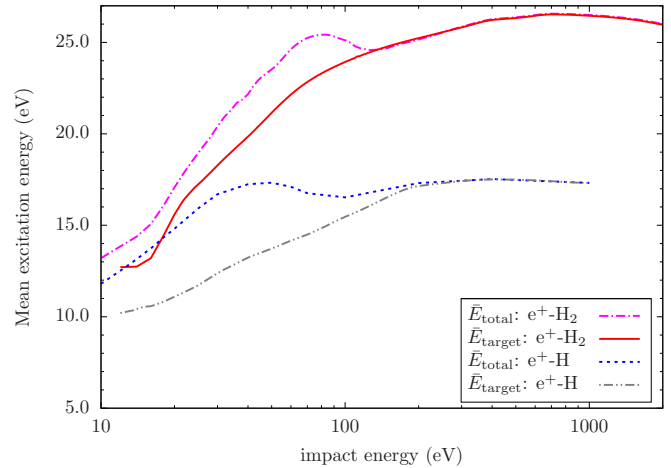


FIG. 8. Mean excitation energies. The results for e^+ -H are obtained from the CCC data of Kadyrov and Bray [66].

studies. Note that positron-impact ionization would not suffer from indistinguishability of projectiles and ejected electrons. Therefore measurements of \bar{E} for positron impact would be desirable.

Figure 8 compares the total and target mean excitation energies for positron impact on atomic and molecular hydrogen. In both H and H₂ cases, the total mean excitation energies have a shoulder structure with a local minimum at about 100 eV where Ps formation becomes negligible. The origin of this structure is in a large energy loss due to Ps-formation channels. Above 100 eV the total and target mean excitation energies converge. Measurements of energy distributions of positrons and/or secondary electrons for positron collisions would be desirable to test validity of the assumptions made in our calculations.

Note that an often used value of the mean excitation energy of H evaluated from the oscillator-strength spectra is 15 eV [65]. For collision energies above 100 eV, the CCC result calculated with Eq. (9) is about 17 eV. Similarly, the mean excitation energy for the molecular hydrogen obtained from the oscillator-strength spectra is 19.2 eV [65]. The CCC results are around 26 eV at above 100-eV impact energies.

Figure 9 shows the mass stopping power of H₂ calculated with Eq. (3) for positrons with impact energies from 10 eV up to 2 keV. The separate contributions from Ps formation and target electronic excitation (including single ionization) are also presented. Above 20 eV the target contribution to the stopping power is dominated by the target ionization channels. The Ps-formation contribution is comparable to the target stopping power at low energies and becomes negligible above 100 eV. Comparison with the Bethe formula [67] with the logarithmic mean excitation energy $I_{\text{H}_2} = 19.2$ [65] shows good agreement above 50 eV.

Figure 10 shows comparison with the mass stopping power results obtained for atomic hydrogen [66]. This is to check the validity of Bragg's additivity rule [68]. Bragg's additivity rule is the approximation to evaluate stopping power of a complex system as a weighted sum of stopping powers of each constituent. When applied to the H₂ molecule, it states the mass stopping power of H₂ to be the same as for H. It can

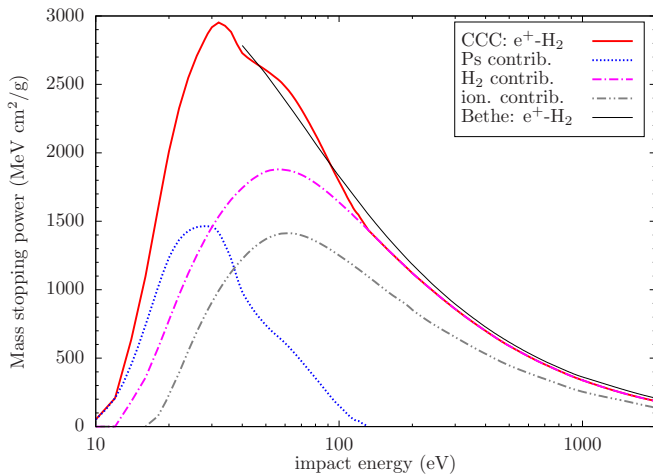


FIG. 9. Positron mass stopping power of H_2 . The contributions due to Ps formation, the total electronic excitations (bound and continuum states), and ionization of H_2 are shown. The Bethe formula results are calculated with the logarithmic mean excitation energy $I_{H_2} = 19.2$ eV [65].

be seen that Bragg's rule is only a valid approximation starting from about 100 eV.

To demonstrate the differences and similarities between positron and electron collisions, in Fig. 11 we compare mass stopping powers of H_2 for positrons and electrons. The CCC calculations for e^-H_2 are from Fursa *et al.* [44]. The experimental data for e^-H_2 are from Munoz *et al.* [63] but modified with the correct total inelastic cross sections as described in Ref. [44]. It can be seen that positron stopping power is larger than for electrons below 1-keV impact energies. This agrees with the observations that positive charged particles travel less distance in media than their negative charged antiparticles [69]. This difference, called the Barkas effect [70], is attributed to different interaction mechanisms [71].

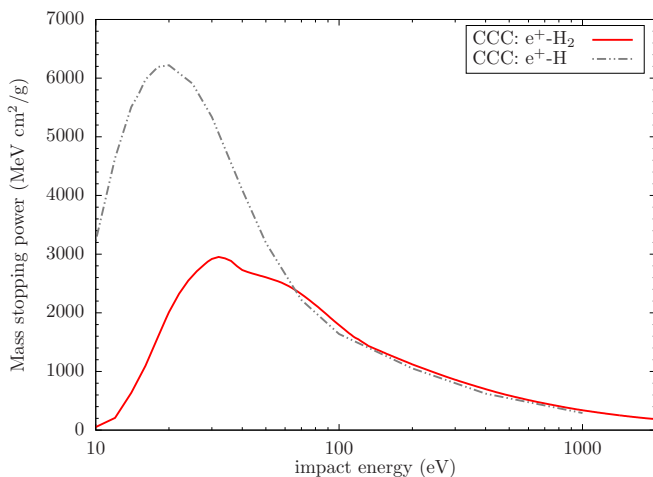


FIG. 10. The CCC results for positron mass stopping powers of atomic and molecular hydrogen. The results for e^+H are obtained from the CCC data of Kadyrov and Bray [66].

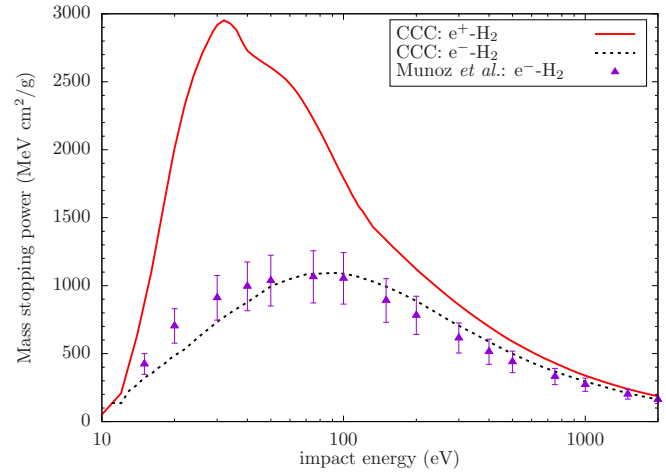


FIG. 11. Mass stopping powers for electrons and positrons. The CCC calculations for e^-H_2 are due to Fursa *et al.* [44] and the experimental data for e^-H_2 are due to Munoz *et al.* [63].

Another noticeable difference is that the maximum of the mass stopping power is at lower energies for positrons at around 30 eV compared to around 70 eV for electrons. This is due to the energy loss to the Ps-formation channels. It can be seen from Fig. 9 that H_2 contribution is peaked at around 70 eV for the positron, similar to the electron case, while the Ps-formation contribution has maxima at lower energies. At above 1-keV energies both positron and electron results are the same within our model, which does not take into account spin-spin interactions and radiative energy-loss processes.

III. CONCLUSIONS

Positron-impact electronic excitations of the H_2 molecule were calculated within the CCC method using the single- and two-center expansions. This provides a detailed set of excitation cross sections for positron- H_2 excitation processes that we hope will be useful in various model studies. The comparison of the CCC results for mass stopping powers of atomic and molecular hydrogen targets shows that Bragg's additivity rule is a good approximation for H_2 only at impact energies above 100 eV. At lower energies the target electronic structure effects need to be taken into account.

ACKNOWLEDGMENTS

This work was supported by the Australian Research Council. We are grateful for access to the Australian National Computing Infrastructure Facility and the Pawsey Supercomputing Centre in Western Australia. A.S.K. acknowledges partial support from the United States National Science Foundation under Award No. PHY-1415656. M.C.Z. would like to specifically acknowledge LANL's ASC PEM Atomic Physics Project for its support. Los Alamos National Laboratory (LANL) is operated by Triad National Security, LLC, for the National Nuclear Security Administration of the U.S. Department of Energy under Contract No. 89233218NCA000001.

- [1] A. David, G. Kögel, P. Sperr, and W. Triftshäuser, *Phys. Rev. Lett.* **87**, 067402 (2001).
- [2] D. Bailey, D. Townsend, P. Valk, and M. Maisey, *Positron Emission Tomography* (Springer, New York, 2005).
- [3] N. Guessoum, *Eur. Phys. J. D* **68**, 1 (2014).
- [4] D. W. Fitzakerley *et al.* (ATRAP Collaboration), *J. Phys. B* **49**, 064001 (2016).
- [5] A. E. Charman *et al.* (ALPHA Collaboration), *Nat. Commun.* **4**, 1785 (2013).
- [6] A. S. Kadyrov, I. Bray, M. Charlton, and I. I. Fabrikant, *Nat. Commun.* **8**, 1544 (2017).
- [7] G. J. Fishman, *Eos* **92**, 185 (2011).
- [8] G. B. Field, W. B. Somerville, and K. Dressler, *Annu. Rev. Astron. Astrophys.* **4**, 207 (1966).
- [9] M. J. Brunger and S. J. Buckman, *Phys. Rep.* **357**, 215 (2002).
- [10] M. C. Zammit, J. S. Savage, D. V. Fursa, and I. Bray, *Phys. Rev. A* **95**, 022708 (2017).
- [11] J. P. Sullivan, A. Jones, P. Caradonna, C. Makochekeanwa, and S. J. Buckman, *Rev. Sci. Instrum.* **79**, 113105 (2008).
- [12] F. Rohrllich and B. C. Carlson, *Phys. Rev.* **93**, 38 (1954).
- [13] R. Batra, *Nucl. Instr. and Meth. B* **28**, 195 (1987).
- [14] W. Bragg and R. Kleeman, *Phil. Mag.* **10**, 318 (1905).
- [15] F. Blanco, A. Muñoz, D. Almeida, F. Ferreira da Silva, P. Limão-Vieira, M. C. Fuss, A. G. Sanz, and G. García, *Eur. Phys. J. D* **67**, 199 (2013).
- [16] R. White, W. Tattersall, G. Boyle, R. Robson, S. Dujko, Z. Petrovic, A. Bankovic, M. Brunger, J. Sullivan, S. Buckman *et al.*, *Appl. Radiat. Isot.* **83**, 77 (2014).
- [17] G. J. Boyle, W. J. Tattersall, D. G. Cocks, S. Dujko, and R. D. White, *Phys. Rev. A* **91**, 052710 (2015).
- [18] H. Gumus, T. Namdar, and A. Bentabet, *IJMBOA* **3** (2018).
- [19] J. G. Lodge, J. W. Darewych, and R. P. McEachran, *Can. J. Phys.* **49**, 13 (1971).
- [20] A. Ray, P. P. Ray, and B. C. Saha, *J. Phys. B: At. Mol. Opt. Phys.* **13**, 4509 (1980).
- [21] E. A. G. Armour, D. J. Baker, and M. Plummer, *J. Phys. B: At. Mol. Opt. Phys.* **23**, 3057 (1990).
- [22] P. K. Biswas, T. Mukherjee, and A. S. Ghosh, *J. Phys. B: At. Mol. Opt. Phys.* **24**, 2601 (1991).
- [23] T. Mukherjee, S. Sur, and A. S. Ghosh, *J. Phys. B: At. Mol. Opt. Phys.* **24**, 1449 (1991).
- [24] R. I. Campeanu, J. W. Darewych, and A. D. Stauffer, *J. Phys. B: At. Mol. Opt. Phys.* **30**, 5033 (1997).
- [25] R. Campeanu and N. Z. Haghian, *Eur. Phys. J. D* **66**, 323 (2012).
- [26] A. Benedek and R. I. Campeanu, *J. Phys. B: At. Mol. Opt. Phys.* **40**, 1589 (2007).
- [27] J. Moxom, P. Ashley, and G. Laricchia, *Can. J. Phys.* **74**, 367 (1999).
- [28] A. Kövér and G. Laricchia, *Phys. Rev. Lett.* **80**, 5309 (1998).
- [29] F. Arretche and M. A. P. Lima, *Phys. Rev. A* **74**, 042713 (2006).
- [30] S. d. A. Sanchez and M. A. P. Lima, *Nucl. Instr. and Meth. B* **266**, 447 (2008).
- [31] J.-Y. Zhang, J. Mitroy, and K. Varga, *Phys. Rev. Lett.* **103**, 223202 (2009).
- [32] R. Zhang, K. L. Baluja, J. Franz, and J. Tennyson, *J. Phys. B: At. Mol. Opt. Phys.* **44**, 035203 (2011).
- [33] J. P. Sullivan, J. P. Marler, S. J. Gilbert, S. J. Buckman, and C. M. Surko, *Phys. Rev. Lett.* **87**, 073201 (2001).
- [34] A. Zecca, L. Chiari, A. Sarkar, K. L. Nixon, and M. J. Brunger, *Phys. Rev. A* **80**, 032702 (2009).
- [35] J. R. Machacek, E. K. Anderson, C. Makochekeanwa, S. J. Buckman, and J. P. Sullivan, *Phys. Rev. A* **88**, 042715 (2013).
- [36] I. Bray, I. B. Abdurakhmanov, J. J. Bailey, A. W. Bray, D. V. Fursa, A. S. Kadyrov, C. M. Rawlins, J. S. Savage, A. T. Stelbovics, and M. C. Zammit, *J. Phys. B: At. Mol. Opt. Phys.* **50**, 202001 (2017).
- [37] M. C. Zammit, D. V. Fursa, J. S. Savage, I. Bray, L. Chiari, A. Zecca, and M. J. Brunger, *Phys. Rev. A* **95**, 022707 (2017).
- [38] R. Utamuratov, A. S. Kadyrov, D. V. Fursa, M. C. Zammit, and I. Bray, *Phys. Rev. A* **92**, 032707 (2015).
- [39] A. S. Kadyrov and I. Bray, *J. Phys. B: At. Mol. Opt. Phys.* **49**, 222002 (2016).
- [40] J. J. Bailey, A. S. Kadyrov, I. B. Abdurakhmanov, and I. Bray, *J. Phys. Conf. Ser.* **777**, 012010 (2017).
- [41] J. Bailey, A. Kadyrov, I. Abdurakhmanov, D. Fursa, and I. Bray, *Phys. Med.* **32**, 1827 (2016).
- [42] J. J. Bailey, A. S. Kadyrov, I. B. Abdurakhmanov, D. V. Fursa, and I. Bray, *Phys. Rev. A* **92**, 052711 (2015).
- [43] J. J. Bailey, A. S. Kadyrov, I. B. Abdurakhmanov, D. V. Fursa, and I. Bray, *Phys. Rev. A* **92**, 022707 (2015).
- [44] D. V. Fursa, M. C. Zammit, R. L. Threlfall, J. S. Savage, and I. Bray, *Phys. Rev. A* **96**, 022709 (2017).
- [45] M. C. Zammit, D. V. Fursa, J. S. Savage, and I. Bray, *J. Phys. B: At. Mol. Opt. Phys.* **50**, 123001 (2017).
- [46] I. Bray and A. T. Stelbovics, *Phys. Rev. A* **46**, 6995 (1992).
- [47] A. W. Bray, I. B. Abdurakhmanov, A. S. Kadyrov, D. V. Fursa, and I. Bray, *Comp. Phys. Comm.* **196**, 276 (2015).
- [48] A. W. Bray, I. B. Abdurakhmanov, A. S. Kadyrov, D. V. Fursa, and I. Bray, *Comp. Phys. Comm.* **203**, 147 (2016).
- [49] M. C. Zammit, D. V. Fursa, and I. Bray, *Phys. Rev. A* **87**, 020701(R) (2013).
- [50] M. Charlton and J. W. Humberston, *Positron Physics* (Cambridge University, Cambridge, England, 2001).
- [51] K. R. Hoffman, M. S. Dababneh, Y. F. Hsieh, W. E. Kauppila, V. Pol, J. H. Smart, and T. S. Stein, *Phys. Rev. A* **25**, 1393 (1982).
- [52] D. Fromme, G. Kruse, W. Raith, and G. Sinapius, *J. Phys. B: At. Mol. Opt. Phys.* **21**, L261 (1988).
- [53] M. C. Zammit, D. V. Fursa, and I. Bray, *J. Phys. Conf. Ser.* **635**, 012009 (2015).
- [54] W. Kolos, K. Szalewicz, and H. J. Monkhorst, *J. Chem. Phys.* **84**, 3278 (1986).
- [55] L. Wolniewicz and K. Dressler, *J. Chem. Phys.* **88**, 3861 (1988).
- [56] J. W. Liu and S. Hagstrom, *Phys. Rev. A* **48**, 166 (1993).
- [57] L. Wolniewicz, *J. Mol. Spectrosc.* **169**, 329 (1995).
- [58] L. Wolniewicz, *J. Mol. Spectrosc.* **174**, 132 (1995).
- [59] L. Wolniewicz and K. Dressler, *J. Chem. Phys.* **100**, 444 (1994).
- [60] L. I. Weiss, A. S. F. Pinho, S. E. Michelin, and M. M. Fujimoto, *Eur. Phys. J. D* **72**, 35 (2018).
- [61] J. L. S. Lino, *Phys. Scr.* **80**, 065303 (2009).
- [62] J. Wrkich, D. Mathews, I. Kanik, S. Trajmar, and M. A. Khakoo, *J. Phys. B: At. Mol. Opt. Phys.* **35**, 4695 (2002).
- [63] A. Munoz, J. C. Oller, F. Blanco, J. D. Gorfinkiel, and G. García, *Chem. Phys. Lett.* **433**, 253 (2007).
- [64] A. Williard, P. Kendall, F. Blanco, P. Tegeder, G. G. García, and N. Mason, *Chem. Phys. Lett.* **375**, 39 (2003).

- [65] S. Kamakura, N. Sakamoto, H. Ogawa, H. Tsuchida, and M. Inokuti, *J. Appl. Phys.* **100**, 064905 (2006).
- [66] A. S. Kadyrov and I. Bray, *Phys. Rev. A* **66**, 012710 (2002).
- [67] P. Sigmund, *Particle Penetration and Radiation Effects* (Springer, New York, 2008).
- [68] D. I. Thwaites, *Radiat. Res.* **95**, 495 (1983).
- [69] F. M. Smith, W. Birnbaum, and W. H. Barkas, *Phys. Rev.* **91**, 765 (1953).
- [70] W. H. Barkas, J. N. Dyer, and H. H. Heckman, *Phys. Rev. Lett.* **11**, 26 (1963).
- [71] P. L. Grande and M. Vos, *Phys. Rev. A* **88**, 052901 (2013).